A comparative electrooxidation study on simply prepared nanoparticles in acidic and alkaline media

Mohammad Etesami,

Norita Mohamed*

School of Chemical Sciences,
Universiti Sains Malaysia (USM),
11800 USM, Penang,
Malaysia

Monometallic and bimetallic nanoparticles of Au, Pd, Pt, (gold-palladium) AuPd and (gold-platinum) AuPt were electrodeposited potentiostatistically on pencil graphite (PG) by applying a constant potential of –0.2 V vs. Ag/AgCl (3 M KCl) in an acidic electrolyte. A scanning electron microscope equipped with energy dispersive X-ray spectroscopy (SEM-EDX) and high resolution X-ray diffraction (XRD) which were used for characterization of the fabricated electrodes confirmed that the metallic and bimetallic deposits have nanoscale dimensions. The fabricated electrodes beside the bare PG were used in a comparative study in acidic and alkaline media. Most common fuels that have been used in fuel cells such as the first *n*-alkanols (C1–C4), 2-propanol, the simplest diol (ethylene glycol), triol (glycerol), polyol (D-glucose), aldehyde (formaldehyde), carboxylic acid (formic acid) and benzyl alcohol have been used in this work. The highest catalytic activity was recorded for the electrooxidation of formic acid on PtNPs/PG (0.62 mA cm^{-2}) and AuPtNPs/PG (0.33 mA cm^{-2}) in the acidic medium while the highest current density was achieved in the alkaline medium for 1-propanol by using AuPtNPs/PG (24 mA cm^{-2}) and AuPdNPs/PG (25 mA cm^{-2}) electrodes.

Key words: metallic electrocatalysts, electrooxidation, fuel, acidic medium, alkaline medium

INTRODUCTION

As energy consumption is growing, consideration of supplying accessible, highly efficient and environment-friendly power sources is greater. Fuel cells are remarkable alternatives that transform chemical energy to electricity. Electrooxidation processes to generate higher energy have been always a challenging subject for researchers. The electrooxidation reactions can be carried out in acidic, alkaline and neutral media [1–3]. Many compounds have been used as fuels in fuel cells. Alcohols such as methanol [4–6], ethanol [7, 8], ethylene glycol [7–9], glycerol [7, 10] and glucose [11–13]

are the mostly-used fuels for fuel cells. Amongst the fuels, methanol and ethanol have been used more as fuels, despite their toxicity and volatility [14]. Electrooxidation of 1-propanol [15, 16], 2-propanol [16, 17] and 1-butanol [18] have also been studied. Ethylene glycol, glycerol and glucose are the simplest diol, triol and polyol, respectively, that have received much attention in fuel cells and catalysis because they are less volatile and toxic (compared to ethanol and methanol) [19]. Besides alcohols, much interest has been devoted to other compounds as fuels such as urea [20], formic acid [21], formaldehyde [22]. Efficiency of the fuel cells depends on several factors such as electrode materials and energy generated from the electrooxidation of the fuels. A fuel can be partly or completely oxidized during the electrooxidation

* Corresponding author: E-mail: mnorita@usm.my

process. Complete oxidation of the fuels is not easy since the C-C bond has to be broken (except for methanol) [23, 24].

Different materials have been used as fuel cell electrodes. A way to increase the efficiency of the electrodes in electrocatalytic processes is to increase the surface area of the electrodes. Nanoparticles are an appropriate choice because of their high surface to volume ratio [25]. Moreover, metallic nanoparticles are more economical alternatives of the bulky metal electrodes. Metallic nanoparticles such as platinum have been used as catalysts for fuel electrooxidation in fuel cells, while non-platinum catalysts have been used as anodes in the fuel cells [1, 5, 12, 16]. Monometallic, bimetallic and multimetallic catalysts can be applied as the anodes in fuel cells for the electrooxidation processes [26, 27]. The monometallic catalysts have unique physicochemical properties. The bimetallic and multimetallic catalysts can be synthesized with different methods to overcome the limitations and drawbacks which exist in monometallic catalysts, for instance, Pt alloys with Ru, Rh and Pb will be less poisonous than monometallic Pt for the electrooxidation of alcohols [28]. Bimetallic catalysts are mostly more active than the monometallic catalysts [24].

Although Au is an inert metal with no vacancies in the 'd' orbital, it can act as a catalyst especially in the alkaline medium. The catalytic performance of Au shows improvement when its alloys are produced [29]. Nanoparticles of Au and Au alloys have been used for electrooxidation of some organic compounds [30–32]. Different methods have been used to synthesize various bimetallic nanoparticles of gold such as Au–Ag [33–35], Au–Cu [36], Au–Fe, Au–Ni, Au–Co [37], Au–Pd [38, 39] and Au–Pt [30, 40]. Electrodeposition is a facile method to synthesize nanoparticles that can be used in catalysis [41, 42].

In the present work, pencil graphite (PG) was used as the working electrode where metallic nanoparticles have been electrodeposited on its surface. PG is a disposable, cost-effective, carbon-based, mechanically rigid and chemically inert material which can be used as a substrate (as bare or modified PG) for electrochemical purposes [43–46].

In this article, we present a simple method via direct electrodeposition to prepare Au, Pd and Pt monometallic electrocatalysts and Au bimetallic nanoparticles with Pd and Pt. The prepared Au, Pd, Pt, AuPd and AuPt nanoparticles were used as the electrodes for the electrooxidation study of some fuels in acidic and alkaline media.

EXPERIMENTAL

Chemicals
$NaAuCl_4$ (99.999%), K_2PdCl_4 (99.99%), K_2PtCl_6 (99.99%), H_2SO_4 (96%), glycerol (99%), ethylene glycol (98%) and glucose (99.5%) were purchased from Sigma-Aldrich. HNO_3, acetone and methanol, ethanol, 1-propanol, 2-propanol, 1-butanol, formic acid, formaldehyde and benzyl alcohol were of analytical grade. All chemicals were freshly used

as received. All glassware was soaked in a solution of 10% (v/v) nitric acid for 24 h. The glassware was then washed with distilled water. All experiments were carried out at room temperature.

Instrumentation
An eDAQ EA 161 potentiostat (linked to an e-corder 410) was used for electrochemical experiments. A three-electrode cell was used for the electrochemical experiments in which pencil graphite (PG, Unicorn Stationery Agency Sdn Bhd, Malaysia), Pt wire and Ag/AgCl (KCl 3 M) were used as the working, counter and reference electrodes, respectively.

To observe morphology of the pencil graphite (PG) and metallic particles electrodeposited on PG, a scanning electron microscope (SEM, Leo Supra 50 VP) equipped with energy dispersive X-ray spectroscopy (EDX) was used.

A high resolution X-ray diffractometer (XRD, PANalytical X'pert PRO MRD Pw 3040) using Cu-$K\alpha1$ radiation ($\lambda = 1.54056$ Å) with a Ni filter working at 40 kV and 30 mA was used to characterize the structure of the prepared electrodes.

Preparation of metallic nanoparticles / PG electrodes
PG (exposed surface area 0.67 cm²) was used for electrochemical experiments after rinsing with acetone and then sonicated in ethanol and distilled water (18 MΩ cm) for 10 min each. To deposit metallic particles on the surface of the PG, the three-electrode system was immersed in the deposition solution. The deposition solution was 0.5 M H_2SO_4 solution containing 1.0 mM $NaAuCl_4$, 1.0 mM K_2PtCl_6, 1.0 mM K_2PdCl_4, 1.0 mM $NaAuCl_4$ + 1.0 mM K_2PdCl_4 and 1.0 mM $NaAuCl_4$ + 1.0 mM K_2PtCl_6 to deposit gold nanoparticles (AuNPs), platinum nanoparticles (PtNPs), palladium nanoparticles (PdNPs), gold-palladium nanoparticles (AuPdNPs) and gold-platinum nanoparticles (AuPtNPs) on the surface of PG. A constant potential of –200 mV was applied for 120 s to deposit metallic particles on PG. N_2 gas was purged into the solution 20 min before each experiment and the N_2 gas was flowed over the solution during the experiments.

RESULTS AND DISCUSSION

Characterization of metallic nanoparticles / PG
The prepared metallic nanoparticles were electrochemically characterized by cyclic voltammetry. The electrochemical surface area (ECSA) values that were calculated from cyclic voltammograms (Fig. 1) are presented. ECSA was calculated by dividing the average charges of gold oxide reduction, palladium oxide reduction and hydrogen adsorption / desorption (after subtraction from the background charge) by 400 $\mu C\ cm^{-2}$, 424 $\mu C\ cm^{-2}$ and 210 $\mu C\ cm^{-2}$ as their reported constants [47–49]. The ECSA of AuNPs (1.43 cm²), PdNPs (4.85 cm²), PtNPs (4.79 cm²), AuPdNPs (7.74 cm²) and AuPtNPs (6.54 cm²) was calculated.
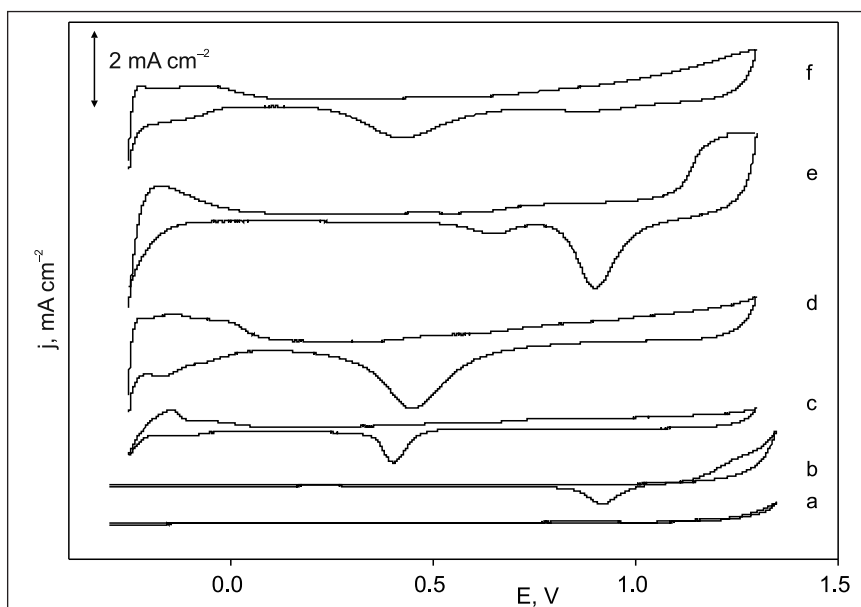
Fig. 1. Cyclic voltammograms of (a) PG, (b) AuNPs/PG, (c) PdNPs/PG, (d) PtNPs/PG, (e) AuPdNPs/PG and (f) AuPtNPs/PG in 0.5 M H_2SO_4 saturated with N_2 gas at scan rate of 100 mV s^{-1}

SEM-EDX and XRD were used for characterization of the prepared electrodes. Fig. 2(a–f) presents SEM micrographs of the bare PG and metallic deposits. EDX analyses of AuPd and AuPt nanoparticles that indicate the existence of two constituents in bimetallic nanoparticles (Fig. 2g and 2h) and XRD patterns of the prepared metallic electrodes (Fig. 2i) were also presented. The amount of monometallic deposits electrodeposited on the surface of the PG electrode was calculated from the integrated charge that was consumed during the electrodeposition:

$$m = \frac{QM}{nF},\qquad(1)$$

where Q (C), m (g), M (g mol^{-1}), n and F (96 487 C mol^{-1}) are the transferred charge during electrodeposition of metallic deposits, the amount of the electrodeposited metal, the molar mass of the electrodeposited metal, number of electrons as-

sociated in the reaction and the Faraday constant, respectively (Table). The crystallite size and d-spacing of the particles calculated from the Scherrer's equation and the XRD data are shown in the Table. The parameters obtained from XRD data indicate that the nanosized alloy crystallites of gold-platinum and gold-palladium were electrodeposited on the surface of PG. As it is shown in Fig. 2i, the (111) peaks related to the bimetallic nanoparticles are located between their monometallic constituents. The position of the (111) facet in AuPd-NPs at 2-theta of 39.18° is located between AuNPs (38.21°) and PdNPs (40.09°) while in AuPtNPs (39.01°) it is between AuNPs and PtNPs (39.82°). Also it can be seen in the Table that the d-spacing of bimetallic nanoparticles is between the constituent monometallic phases. The positions of (111) facets of bimetallic nanoparticles confirm the formation of alloy phases [50]. According to Vegard's law [51], the lattice parameters of alloys vary linearly with their compositions.

Table. **The amount of electrodeposited metal was calculated from the transferred charge during electrodeposition. Crystallite size and d-spacing of synthesized electrocatalysts are based on the XRD data and calculated from Scherrer's equation corresponding to the (111) peak of nanoparticles**

Electrode	Q, mC[i]	Q_{net}, mC[ii]	n, μmol[iii]	m, μg[iv]	2-theta, degree	d-spacing, nm	d, nm[v]
PG	5.176	–	–	–	–	–	–
AuNPs	21.134	15.958	0.1654	10.859	38.21	0.2355	55.00
PdNPs	26.574	21.398	0.2218	11.800	40.09	0.2249	72.26
PtNPs	27.53	22.354	0.2317	11.299	39.82	0.2264	81.44
AuPdNPs	43.564	38.388	0.3979	–	39.18	0.2299	72.07
AuPtNPs	45.302	40.126	0.4159	–	39.01	0.2309	50.33

[i] Q: total amount of transferred charge during electrodeposition of metallic electrocatalysts, calculated from integrated i vs t.

[ii] Q_{net}: amount of transferred charge after subtracting blank solution.

[iii] $n = \frac{Q}{F}$, n: electron transferred, F: Faraday constant (96487 C mol^{-1}).

[iv] Amount of catalyst loading on the surface of PG based on the amount of transferred charge during electrodeposition according to Faraday's law.

[v] Calculated from Scherrer's equation ($d = \frac{K\lambda}{\beta \cos\theta}$, $K = 0.89$, d: crystallite size, λ: wave length, β: full width at half maximum, θ: scattering angle.
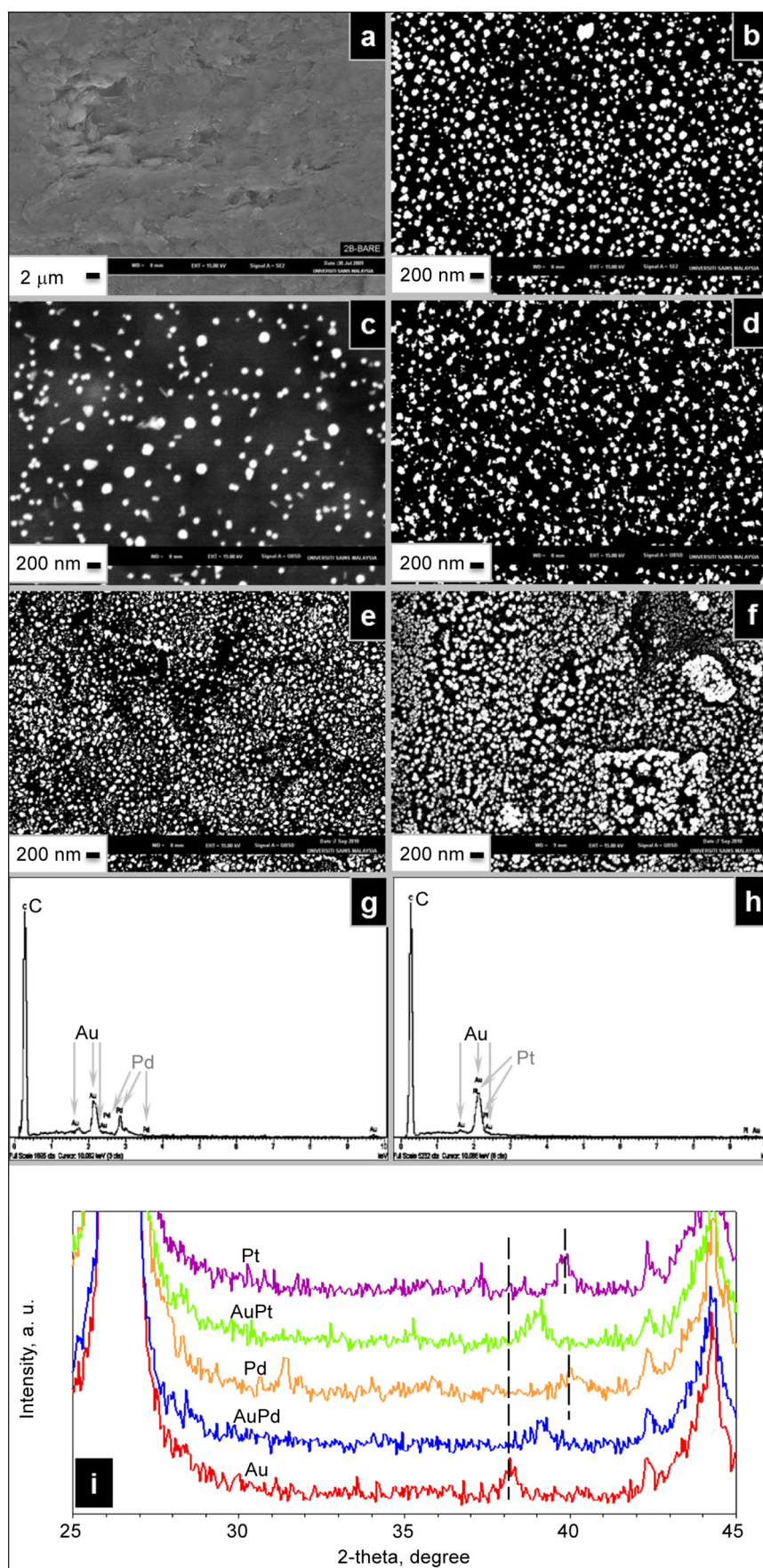
Fig. 2. SEM images of (a) bare PG, (b) AuNPs/PG, (c) PdNPs/PG, (d) PtNPs/PG, (e) AuPdNPs/PG and (f) AuPtNPs/PG. EDX analyses of (g) AuPd and (h) AuPt electrocatalysts. (i) XRD patterns of the metallic electrocatalysts on the PG

The lattice parameter of the alloy can be calculated as follows:

$$a_{alloy} = x_A a_A + (1 - x_A) \, a_B, \tag{2}$$

where x and a are the atomic fraction and lattice parameter of constituents A and B, respectively. According to Vegard's law, the compositions of the prepared bimetallic alloys were estimated to ca. $Au_{0.47}Pd_{0.53}$ and $Au_{0.49}Pt_{0.51}$ which were calculated from the lattice parameters (calculated from d-spacings in the cubic structure) of the (111) facet (Table). The nominal compositions for Au:Pd and Au:Pt in the deposition solutions were 1 : 1 according to the atomic ratio. The data obtained from the XRD data indicated that the composition of Au and Pt atoms in AuPt deposits is very close to the nominal composition of Au and Pt atoms in the deposition solution. Thus, Au and Pt atoms are completely (homogeneously) dispersed in the AuPt alloy. In the AuPd alloy, Au and Pd atoms are almost homogeneously mixed in the alloy while some of the Pd atoms have been formed in a single phase [52].

Electrooxidation of several fuels in acidic and alkaline media

The electrooxidation of several organic compounds used as fuels in acidic and alkaline electrolytes was investigated using the electrodeposited metallic nanoparticles on PG. The specific range of the potential was chosen in each acidic and alkaline media for the electrooxidation processes, such that in the applied conditions no leaching of the heterogeneous catalysts should be seen in the liquid electrolyte [53].

Acidic medium

Electrooxidation of the first saturated aliphatic alcohols (C1–C4), the simplest carboxylic acid, aldehyde, diol, triol and polyol beside benzyl alcohol was investigated by cyclic voltammetry in an acidic medium. All experiments were carried out in 0.1 M H_2SO_4 containing 0.1 M of the above-mentioned fuels. As an instance, the electrooxidation of benzyl alcohol in 0.1 M H_2SO_4 is shown in Fig. 3 using the bare PG and different metal deposited PG electrodes. Some catalysts are active or inactive in a medium such as gold which is inactive in acidic electrolytes. Platinum is an active catalyst in an acidic electrolyte [54]. As it is shown in Fig. 3, the PG electrode shows activity to the acidic electrolyte containing benzyl alcohol. Despite few works that were conducted on the electrooxidation of benzyl alcohol in acidic medium [55, 56], the bare and metallic nanoparticles (except Au) were highly active when exposed to the acidic solution of benzyl alcohol. As shown, benzyl alcohol can be oxidized over PG (Fig. 3a). Gold nanoparticles showed no activity toward electrooxidation of benzyl alcohol (Fig. 3b). Gold is not a good catalyst in acidic media. Indeed, gold can oxidize aldehydes to their relative carboxylic acids but it is unable to oxidise alcohols to aldehydes [57]. The oxide form of palladium is produced when the potential is swept towards positive potentials as indicated in Fig. 3c (dotted line) or due to the partial surface oxidation of the as-prepared catalyst [58] or chemisorption of oxygen on the surface [59]. As the catalyst is exposed to benzyl alcohol, the palladium oxide species may be reduced to metallic palladium by the benzyl alcohol which is being oxidised. The number of palladium oxide species is lower at more positive potentials which corresponds to a decrease in the peak current from 360 mV onwards compared to that for PdNPs exposed to the electrolyte without benzyl alcohol. Fig. 3d, which shows the catalytic performance of platinum, indicates that Pt is a highly active catalyst for the electrooxidation of benzyl alcohol. Different electronegativities and activities of palladium and platinum affect the activity of gold bimetallic catalysts compared to gold that has low activity in acidic media [60]. Cyclic voltammograms of the AuPd and
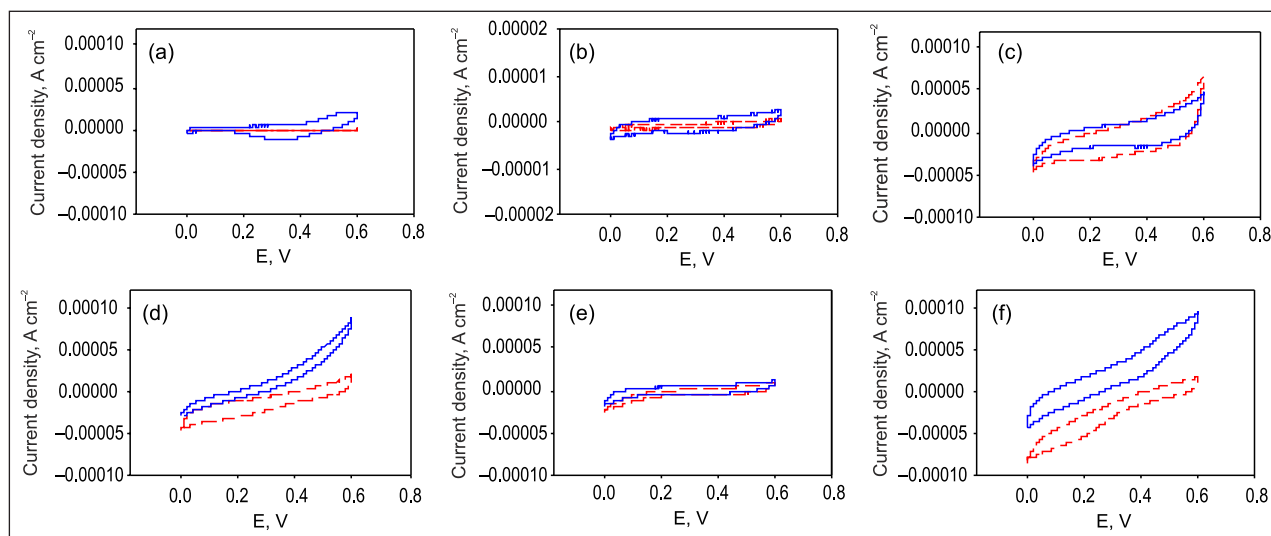

Fig. 3. Cyclic voltammograms of 0.1 M H_2SO_4 (dotted line) containing 0.1 M benzyl alcohol (solid line) on (a) PG, (b) AuNPs/PG, (c) PdNPs/PG, (d) PtNPs/PG, (e) AuPdNPs/PG and (f) AuPtNPs/PG electrodes at scan rate of 100 mV s^{-1}

Fig. 4. Multibar chart of the electrooxidation peak current densities of several fuel compounds on different electrodes in 0.1 M H₂SO₄. The peak current densities were obtained by sweeping potential in the range of 0 mV–600 mV at scan rate of 100 mV s⁻¹
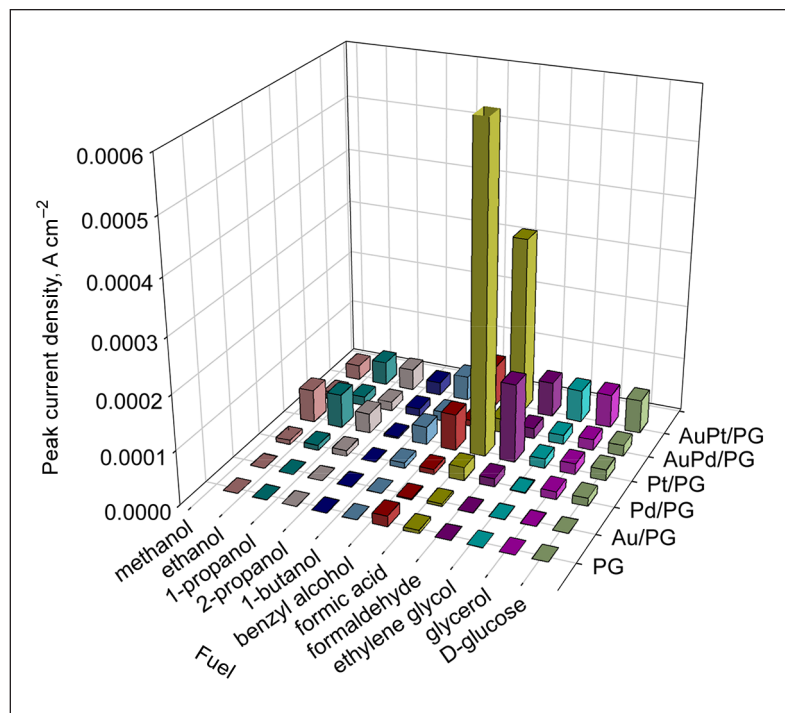
AuPt electrocatalysts toward the electrooxidation of benzyl alcohol are shown in Fig. 3e and 3f. As can be seen in the Figures, the AuPt electrocatalysts are more active than AuPd-NPs. The species that was generated as the result of the electrooxidation of benzyl alcohol during the positive-going scan can be significantly oxidized in the negative-going scan on PtNPs and AuPtNPs.

To evaluate the catalytic performance of the electrodes in the solution containing fuels, the current density obtained with an electrode in supporting electrolyte was subtracted from the current density obtained with that electrode in the supporting electrolyte containing the fuels. Since it would be erroneous to compare the current densities at a specific potential, the subtraction was applied in the potential range during the positive-going scan. The electrooxidation of different organic compounds was conducted on the electrodeposited metallic electrocatalysts and the bare PG using cyclic voltammetry in an identical potential range, scan rate (100 mV s⁻¹) in the acidic medium (Fig. 4). PG is not an active substrate for the electrooxidation process (except for benzyl alcohol). Gold is not an appropriate catalyst in acidic media since no catalytic activity was observed with the fuels. In this medium, PtNPs and AuPtNPs performed better than PdNPs and AuPdNPs. Pt electrocatalysts indicated catalytic activity to all fuels but the activity of PtNPs to electrooxidation of 2-propanol is negligible as was also reported in acidic medium using online differential electrochemical mass spectroscopy (DEMS) [61]. This is due to prevention of the reaction to produce acetone but the catalytic activity of PtNPs improved in Pt bimetallic catalysts [15] as was observed for AuPt electrocatalysts. Pt and AuPt electrocatalysts exhibit higher catalytic activity when exposed to formic acid (0.62 mA cm⁻² and 0.33 mA cm⁻² respectively).

Alkaline medium

Electrooxidation of the fuels was studied on the prepared electrodes in alkaline electrolyte by cyclic voltammetry. As reported [2, 14, 62], catalysts usually depict higher performance in alkaline electrolytes than acidic solutions. To compare the data obtained from the alkaline electrolyte with the data obtained from the acidic medium, the solution of 0.1 M NaOH containing 0.1 M fuel was used for the electrooxidation processes. The electrooxidation of D-(+)-glucose (0.1 M) in 0.1 M NaOH is shown in Fig. 5 as an example. Alkaline electrolytes are a better medium for the electrooxidation process of alcohols. As can be seen in Fig. 5a, the bare PG electrode is not active in the alkaline electrolyte containing D-glucose. AuNPs exhibited higher activity in alkaline electrolytes than in acidic medium. D-glucose was oxidized on the metallic and bimetallic electrocatalysts during the positive-going scan and the generated species was oxidized during the negative-going scan. As reported, PdO or PdOH [48, 63], the metal oxide layer of gold [64] and platinum [65] play an important role in the reoxidation peak in the negative-going scan. The oxidation peak in the positive-going scan and the reoxidation peak in the negative-going scan were higher for AuPdNPs and AuPtNPs than for AuNPs, PdNPs and PtNPs due to the fact that the bimetallic catalysts generally perform better in the electrooxidation processes compared to their monometallic constituents [29].

The electrooxidation of the afore-mentioned fuels in the alkaline medium was studied in an identical condition (potential range of –600–800 mV at scan rate of 100 mV s⁻¹) on the bare PG and metallic nanoparticles electrodeposited on the PG electrodes by cyclic voltammetry. The background current (recorded in 0.1 M NaOH) was substracted from
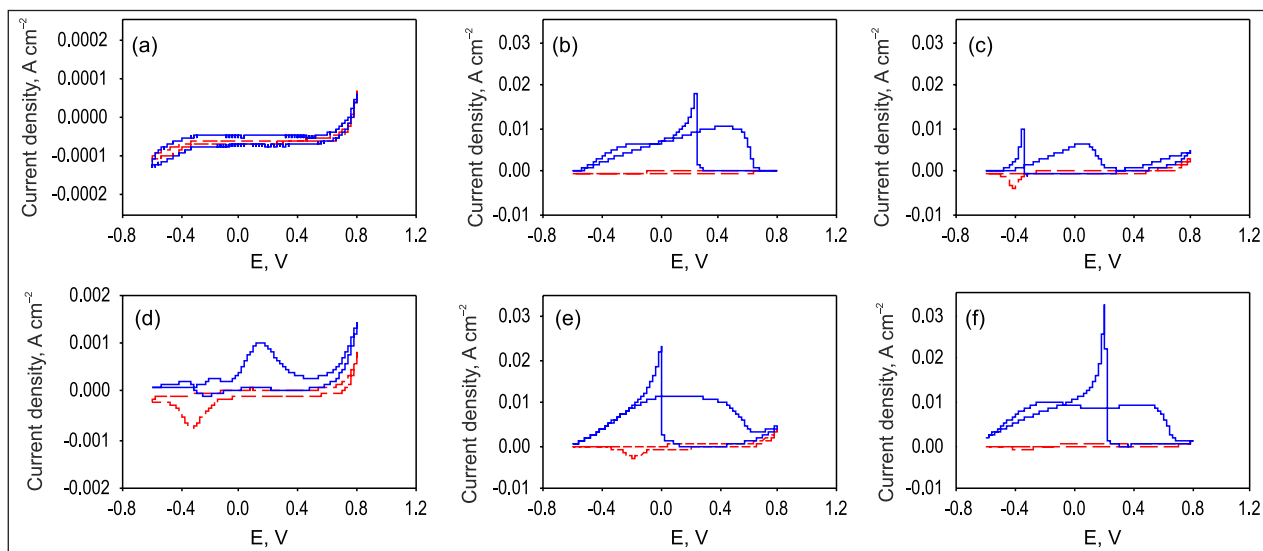
Fig. 5. Cyclic voltammograms of 0.1 M NaOH (dotted line) containing 0.1 M, D-(+)-glucose (solid line) on (a) PG, (b) AuNPs/PG, (c) PdNPs/PG, (d) PtNPs/PG, (e) AuPdNPs/PG and (f) AuPtNPs/PG electrodes at scan rate of 100 mV s⁻¹

the peak current density (recorded in 0.1 M NaOH + 0.1 M fuel) generated by each electrode in the alkaline medium (Fig. 6). The PG electrode is not active in this medium since no activity was observed in the alkaline medium containing fuels. The ability of the metal catalyst to adsorb organic compounds is a key factor in the electrooxidation processes. Gold is an active electrocatalyst in alkaline medium by adsorbing hydroxyl groups to facilitate the facile electrooxidation reactions [66]. However, methanol is not an appropriate fuel on gold because there is no adsorption [4] or adsorption is weak on a specific orientation of gold [67]. The gold electrocatalysts showed higher activity to the oxidation of glycerol, D-glucose, formaldehyde and benzyl alcohol than other fuels because of

better catalytic performance of gold in this medium. In the medium with enough hydroxyl species, palladium atoms aid the oxidation reaction [24]. The Pd electrocatalysts demonstrated catalytic activities to all the afore-mentioned fuels. The best catalytic activity of the Pd electrocatalysts was attributed to formaldehyde. The Pt electrocatalysts indicated higher activity to formaldehyde, ethylene glycol and glycerol than other fuels. Negligible activity was seen for the Pt electrocatalysts toward the electrooxidation of 2-propanol and benzyl alcohol. The synthesized bimetallic electrocatalysts (AuPd and AuPt) are intriguing materials as anodes in fuel cells due to their high catalytic performance. As can be seen in Fig. 6, the bimetallic catalysts are active to the electrooxi-
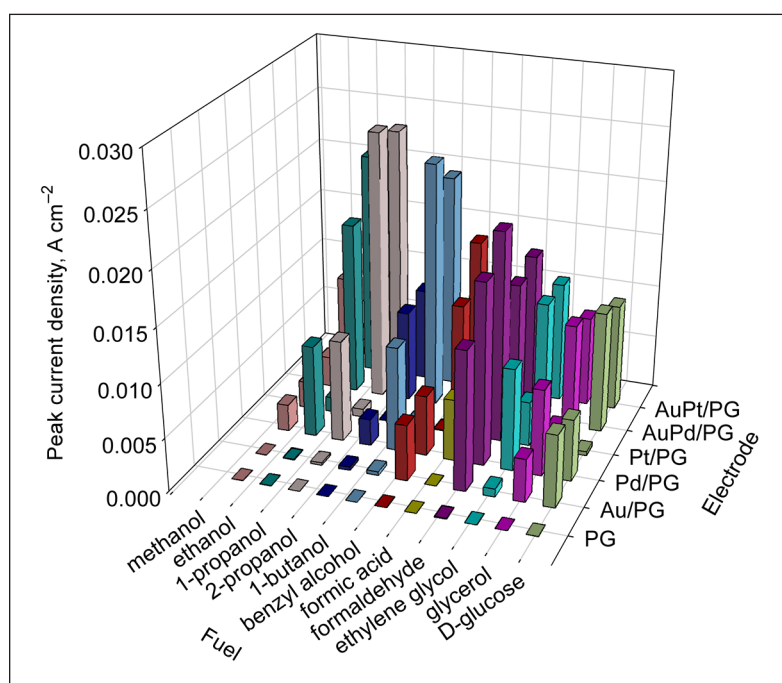

Fig. 6. Multibar chart of the electrooxidation peak current densities of several fuel compounds on different electrodes in 0.1 M NaOH. The peak current densities were obtained by sweeping potential in the range of −600–800 mV at scan rate of 100 mV s⁻¹

dation of all mentioned fuels. Amongst all fuels that were used in this study, formaldehyde can be used as an efficient fuel by using the metallic and bimetallic electrodes in alkaline medium since formaldehyde was highly oxidized on all monometallic and bimetallic electrocatalysts (>13 mA cm^{-2}). The highest catalytic activity was recorded for the electrooxidation of 1-propanol on AuPt (24 mA cm^{-2}) and AuPd (25 mA cm^{-2}) catalysts in the alkaline medium. The high catalytic activity of the bimetallic catalysts can be due to different electronegativities between two counterparts since Au (2.54) is more electronegative than Pt (2.28) and Pd (2.2). The difference in electronegativity leads to charge transfer from one component to other counterpart. Besides that, changes in the *d*-spacings and lattice parameters in bimetallic catalysts (compared to pure monometallic counterparts) affect the catalytic performance of bimetallic catalysts [47, 68, 69].

CONCLUSIONS

The Au, Pd, Pt, AuPd and AuPt electrocatalysts were electrodeposited on the pencil graphite (PG) by applying a constant potential in the acidic electrolyte. The electrodes indicated stability during the experiments as no leaching was observed. The bare PG and metallic nanoparticles electrodeposited on the PG electrodes were used in this work to compare the ability of the electrodeposited nanoparticles toward the electrooxidation of the most common fuels in the acidic and alkaline media. PG did not show any activity in the acidic (except to benzyl alcohol) and alkaline media. The catalytic performance of the electrodeposited monometallic and bimetallic nanoparticles varied from medium to medium and fuel to fuel. The fuels mostly present better results in the alkaline medium rather than the acidic electrolyte.

ACKNOWLEDGEMENTS

References

1. P. K. Shen, C. Xu, *Electrochem. Commun.*, **8**, 184 (2006).
2. C. Xu, K. S. Pei, *Chem. Commun.*, **10**, 2238 (2004).
3. B. Wu, Y. Gao, G. Li, W. Qu, Z. Jiang, *Catal. Lett.*, **106**, 167 (2006).
4. M. S. Ureta-Zañartu, A. Alarcón, G. Muñoz, C. Gutiérrez, *Electrochim. Acta*, **52**, 7857 (2007).
5. C. Xu, Y. Hu, J. Rong, S. P. Jiang, Y. Liu, *Electrochem. Commun.*, **9**, 2009 (2007).
6. Y. Xu, S. Lin, X. Peng, W. A. Luo, J. Y. Gal, L. Dai, *Sci. China Chem.*, **53**, 2006 (2010).
7. C. Xu, Z. Tian, P. Shen, S. P. Jiang, *Electrochim. Acta*, **53**, 2610 (2008).
8. J. Sieben, M. Duarte, C. Mayer, J. Bazán, *J. Appl. Electrochem.*, **39**, 1045 (2009).
9. M. Etesami, N. Mohamed, *Sci. China Chem.*, **55**, 247 (2012).
10. L. Su, W. Jia, A. Schempf, Y. Lei, *Electrochem. Commun.*, **11**, 2199 (2009).
11. M. Pasta, F. La Mantia, Y. Cui, *Electrochim. Acta*, **55**, 5561 (2010).
12. X. Yan, X. Ge, S. Cui, *Nanoscale Res. Lett.*, **6**, 313 (2011).
13. M. W. Hsiao, R. R. Adzic, E. B. Yeager, *J. Electrochem. Soc.*, **143**, 759 (1996).
14. C. Xu, R. Zeng, P. K. Shen, Z. Wei, *Electrochim. Acta*, **51**, 1031 (2005).
15. I. D. A. Rodrigues, J. P. I. De Souza, E. Pastor, F. C. Nart, *Langmuir*, **13**, 6829 (1997).
16. J. Liu, J. Ye, C. Xu, S. P. Jiang, Y. Tong, *J. Power Sources*, **177**, 67 (2008).
17. J. Ye, J. Liu, C. Xu, S. P. Jiang, Y. Tong, *Electrochem. Commun.*, **9**, 2760 (2007).
18. Y. L. Chen, T. C. Chou, *J. Appl. Electrochem.*, **26**, 543 (1996).
19. A. Nirmala Grace, K. Pandian, *Electrochem. Commun.*, **8**, 1340 (2006).
20. R. Lan, S. Tao, J. T. S. Irvine, *Energy Environ. Sci.*, **3**, 438 (2010).
21. I.-S. Park, K.-S. Lee, S. J. Yoo, Y.-H. Cho, Y.-E. Sung, *Electrochim. Acta*, **55**, 4339 (2010).
22. R. Ojani, J. Raoof, S. Zavvarmahalleh, *J. Solid State Electrochem.*, **13**, 1605 (2009).
23. R. L. Arechederra, S. D. Minteer, *Fuel Cells*, **9**, 63 (2009).
24. E. H. Yu, U. Krewer, K. Scott, *Energies*, **3**, 1499 (2010).
25. N. R. Stradiotto, K. E. Toghill, X. Lei, A. Moshar, R. G. Compton, *Electroanalysis*, **21**, 2627 (2009).
26. L. Demarconnay, S. Brimaud, C. Coutanceau, J. M. Léger, *J. Electroanal. Chem.*, **601**, 169 (2007).
27. A. Kelaidopoulou, E. Abelidou, A. Papoutsis, E. K. Polychroniadis, G. Kokkinidis, *J. Appl. Electrochem.*, **28**, 1101 (1998).
28. A. Verma, S. Basu, *J. Power Sources*, **174**, 180 (2007).
29. H. Möller, P. C. Pistorius, *J. Electroanal. Chem.*, **570**, 243 (2004).
30. S. Zhang, Y. Shao, G. Yin, Y. Lin, *J. Power Sources*, **195**, 1103 (2010).
31. A. Habrioux, E. Sibert, K. Servat, W. Vogel, K. B. Kokoh, N. Alonso-Vante, *J. Phys. Chem. B*, **111**, 10329 (2007).
32. F. El-Cheick, F. Rashwan, H. Mahmoud, M. El-Rouby, *J. Solid State Electrochem.*, **14**, 1425 (2010).
33. K. I. Okazaki, T. Kiyama, K. Hirahara, N. Tanaka, S. Kuwabata, T. Torimoto, *Chem. Commun.*, 691 (2008).
34. A. Pal, S. Shah, S. Devi, *Colloids Surf., A*, **302**, 51 (2007).
35. M. Tominaga, T. Shimazoe, M. Nagashima, I. Taniguchi, *J. Electroanal. Chem.*, **615**, 51 (2008).
36. N. E. Motl, E. Ewusi-Annan, I. T. Sines, L. Jensen, R. E. Schaak, *J. Phys. Chem. C*, **114**, 19263 (2010).
37. D.-L. Lu, K. Domen, K.-I. Tanaka, *Langmuir*, **18**, 3226 (2002).

38. Y. Suo, I. M. Hsing, *Electrochim. Acta*, **56**, 2174 (2011).

39. D. Jana, A. Dandapat, G. De, *J. Phys. Chem. C*, **113**, 9101 (2009).

40. F. Xiao, Z. Mo, F. Zhao, B. Zeng, *Electrochem. Commun.*, **10**, 1740 (2008).

41. M. Etesami, F. S. Karoonian, N. Mohamed, *J. Chin. Chem. Soc.*, **58**, 688 (2011).

42. M. Etesami, N. Mohamed, *Int. J. Electrochem. Sci.*, **6**, 4676 (2011).

43. M. Muti, F. Kuralay, A. Erdem, S. Abaci, T. Yumak, A. Sinag, *Talanta*, **82**, 1680 (2010).

44. B. Dogan-Topal, S. A. Ozkan, *Electrochim. Acta*, **56**, 4433 (2011).

45. A. Levent, Y. Yardim, Z. Senturk, *Electrochim. Acta*, **55**, 190 (2009).

46. L. Özcan, Y. Sahin, H. Türk, *Biosens. Bioelectron.*, **24**, 512 (2008).

47. G. Chen, Y. Li D. Wang, et al., *J. Power Sources*, **196**, 8323 (2011).

48. M. Grdeń, M. Łukaszewski, G. Jerkiewicz, A. Czerwiński, *Electrochim. Acta*, **53**, 7583 (2008).

49. S. Trasatti, O. A. Petrii, *Pure Appl. Chem.*, **63**, 711 (1991).

50. S. Pal, G. De, *PCCP*, **10**, 4062 (2008).

51. B. X. Liu, M. A. Nicolet, *Thin Solid Films*, **101**, 201 (1983).

52. M. D. Obradović, J. R. Rogan, B. M. Babić, et al., *J. Power Sources*, **197**, 72 (2012).

53. R. A. Sheldon, M. Wallau, I. W. C. E. Arends, U. Schuchardt, *Acc. Chem. Res.*, **31**, 485 (1998).

54. M. Betowska-Brzezinska, T. Uczak, R. Holze, *J. Appl. Electrochem.*, **27**, 999 (1997).

55. M. J. Gonzalez, C. T. Hable, M. S. Wrighton, *J. Phys. Chem. B*, **102**, 9881 (1998).

56. L. W. H. Leung, M. J. Weaver, *Langmuir*, **6**, 323 (1990).

57. T. Mallat, A. Baiker, *Chem. Rev.*, **104**, 3037 (2004).

58. M. Besson, P. Gallezot, *Catal. Today*, **57**, 127 (2000).

59. R. K. Pandey, V. Lakshminarayanan, *J. Phys. Chem. C*, **113**, 21596 (2009).

60. X. Kang, Z. Mai, X. Zou, P. Cai, J. Mo, *Anal. Biochem.*, **369**, 71 (2007).

61. I. A. Rodrigues, F. C. Nart, *J. Electroanal. Chem.*, **590**, 145 (2006).

62. Y. Chen, L. Zhuang, J. Lu, *Chin. J. Catal.*, **28**, 870 (2007).

63. L.-M. Lu, H.-B. Li, F. Qu, X.-B. Zhang, G.-L. Shen, R.-Q. Yu, *Biosens. Bioelectron.*, **26**, 3500 (2011).

64. M. Pasta, R. Ruffo, E. Falletta, C. M. Mari, C. Della Pina, *Gold Bull.*, **43**, 60 (2010).

65. H.-W. Lei, B. Wu, C.-S. Cha, H. Kita, *J. Electroanal. Chem.*, **382**, 103 (1995).

66. D. Z. Jeffery, G. A. Camara, *Electrochem. Commun.*, **12**, 1129 (2010).

67. Y. Chen, W. Schuhmann, A. W. Hassel, *Electrochem. Commun.*, **11**, 2036 (2009).

68. A. Tegou, S. Armyanov, E. Valova, et al., *J. Electroanal. Chem.*, **634**, 104 (2009).

69. J. Xu, T. White, P. Li, et al., *J. Am. Chem. Soc.*, **132**, 10398 (2010).

Mohammad Etesami, Norita Mohamed

ELEKTROOKSIDACIJOS ANT PAPRASTU BŪDU PARUOŠTŲ NANODALELIŲ TYRIMAS RŪGŠČIOJE IR ŠARMINĖJE TERPĖSE

S a n t r a u k a

Monometalinės Au, Pd ir Pt bei bimetalinės AuPd ir AuPt nanodalelės buvo potenciostatiškai nusodintos iš rūgštaus elektrolito ant pieštuko grafito ir charakterizuotos skenuojančios elektroninės mikroskopijos bei rentgeno spindulių difrakcijos metodais. Paruošti elektrodai pasižymi kataliziniu aktyvumu, elektrochemiškai oksiduojant tam tikrus organinius junginius.